Hindawi
International Transactions on Electrical Energy Systems
Volume 2023, Article ID 1754305, 17 pages
https://doi.org/10.1155/2023/1754305

Research Article

A New Method for Fault Detection and Location in a Low-Resistance Grounded Power Distribution Network Using Voltage Phasor of D-PMUs Data

Masoud Najafzadeh, Jaber Pouladi, Ali Daghigh, Jamal Beiza, and Sima Shahmohamadi

Department of Electrical Engineering, Shabestar Branch, Islamic Azad University, Shabestar, Iran

Correspondence should be addressed to Jaber Pouladi; pouladi.jaber@gmail.com

Received 28 September 2022; Revised 18 November 2022; Accepted 25 May 2023; Published 22 July 2023

Academic Editor: Michele De Santis

Electric power grids are always affected by numerous unexpected faults. Occurrence of these faults will have a negative impact on network availability and reliability indices of the network. But the indicators of reliability and quality of electrical energy in the network can be augmented by locating the fault in the shortest time. Special features of distribution networks such as load and network imbalance, existence of different types of load with different connections, existence of multiphase branches, effects related to different conductors, capacitive effects of distribution lines, and limited numbers of measuring devices complicate the process of fault localization in distribution networks. On the other hand, increasing penetration of distributed generation units has caused conventional methods of fault localization. Therefore, it is mandatory to introduce new methods of fault locating by considering the mentioned features. Hence, in the current study, nonlinear methods are presented for identifying the location of ground faults in the power distribution network with the help of voltage phasor measurement at different network buses by the D-PMU phased distribution unit. In the first technique, the genetic optimization algorithms and particle swarm optimization for nonlinear modeling of fault position along the distribution line have been utilized for different single-phase, two-phase, and three-phase faults, and in the second technique, neural fuzzy network training has been proposed by different phasor measurement devices. In this case, it is enough to access the phase information of the network bus voltage. In order to show the effectiveness of the proposed algorithms, a 9-bus system is defined by MATLAB software and also defining different line lengths and line characteristics in different buses. Moreover, after applying single-phase, two-phase, and three-phase faults, as well as presenting the results, fault localization is detected in the shortest time.

1. Introduction

Nowadays, distribution and super-distribution networks have the highest number of different faults. Thus, the expansion of these networks and also the high volume of recorded information make these systems more complex. Consequently, it is imperative to implement a system in order to perform fault detection at the lowest possible time and with high reliability in distribution networks [1, 2]. The transmission line is an important component of the electrical power system and its protection is essential to ensure the stability of the system and reduce the damage done to the equipment due to a short connection in transmission lines [3–5]. Transmission line relays have three important functions: detecting, classifying, and locating transmission line faults. Fast detection of a transmission line fault facilitates the fast separation of the faulted line from service; hence, it protects the system from harmful effects of the fault [6, 7]. Fault classification is the identification of the type of fault, and this information is essential for locating the fault and assessing the extent of repairs [8]. High accuracy of fault location is essential to facilitate rapid repair and separation of faulty line, improve reliability, and access to power source [9]. Various fault location (FL) schemes have been used in real systems, including phasor-based fault location (PHFL) techniques, which are still the most common [10]. These

solutions require estimation of the basic phases of voltage and current which are used as inputs to the FL formulae. Backup protection may be local, remote, or both [11, 12]. To realize the support of remote sensing protection, the use of phasor measurement units (PMU) has been subject to university and industry attention in several years.

Short circuit faults are common in transmission lines and are the worst type of faults that cause many hazards in lines such as reduced component life, increased power and heat loss of cables, and damage to insulation [13, 14]. Various types of short circuit faults occur during daily work and are mainly classified into two symmetric and asymmetric faults. Symmetric or balanced faults, which keep the system balanced, include three-line ground (LLLG) and triple-line (LLL) lines and are unlikely to occur, but they are the most severe type of short circuit faults, which include large destruction effects and damage to system equipment [15, 16]. Asymmetric or unbalanced faults that unbalance the power system during a fault include two-line ground (LLG), ground-to-line (LG), and line-to-line (LL) lines. Although their intensity is lower compared to balanced rivals, they are of great importance because one-to-ground faults are more than 80% likely to occur [17]. In this work, ground connection faults have been worked on.

In [18–20], smart meters (SMs) are placed in several system buses so that they do not synchronize prefault and fault voltage measurements. From the voltage drop vector, the flow distribution vector is calculated. The substation and all buses of DG have to be equipped with digital fault recorders (DFR). The amount of fault current is obtained through the sum of the currents injected by each DG and the source of the post. Knowing the system impedance matrix and fault current, different voltage drops are calculated for all buses with DG. Since the actual voltage sag is recorded on each bus with DG, the voltage drop calculated with the lowest fault, compared to the actual voltage drop, related to the fault location can be used [21, 22]. Therefore, such a method is based on classical analysis and does not require complicated mathematical techniques and load data; the fault occurrence position can be calculated with the help of voltage drop information at the beginning and end of the transmission line.

In the current study, a new method for locating faults in the distribution network using voltage phase information is introduced. Finding fault location in four stages is accomplished: first, the voltage before and during the fault is received by the phasor measurement equipment installed at the network buses. In the next step, utilizing the values of voltage drop in various phases of the power system, the types of single-phase, two-phase, and three-phase faults are calculated and estimated in proportion to each of these received voltage drops, and the segments with potential for fault are calculated according to the number of buses. In the third stage, using two nonlinear modeling methods using phasor measurement methods in each fault line, fault location for each of the fault types is extracted, and finally, due to the proposed techniques of genetic algorithm and swarm optimization of PSO particles and ANFIS neural fuzzy, the fault event location is achieved relative to the potential bus. In addition, the algorithm utilizes an optimization of the coefficients of the third-order nonlinear model to investigate the range of faults estimated by minimizing the objective function to a detailed model to determine the fault location based on phasor measurement voltages of buses. The proposed method uses intelligent measuring equipment and D-PMU phase-measuring equipment to obtain voltage drooping. Distributed generation and loads were modeled as fixed impedance and then studied in the network. The proposed method is implemented in the IEEE 9 bus test distribution network as well as in the MATLAB simulator environment.

In this work, an endeavor is made to implement fault position detection in distribution networks using neural fuzzy network and optimization algorithms. Due to high volume of information in distribution networks, information monitoring is often encountered problems. Therefore, here, it has been tried to use voltage-phasor measurement information in buses. So, there is no longer the need for complicated mathematical calculations in other methods of fault detection such as impedance methods. Therefore, the phase voltage information is applied directly as input to the estimator system and with nonlinear modeling and according to fixed network information such as length and characteristics of network lines and types of single-phase, two-phase, and three-phase fault positions in the network, fault positions are tracked in the shortest possible time.

The contents of this paper are as follows. In Section 2, the study of the work carried out in the field of detection and positioning of events and faults is discussed in the power distribution network. Section 3 deals with background studies and provides basic concepts. Section 4 describes the proposed algorithms and techniques for accurate positioning and fault type. In Section 4, the 9-bus system studied under the MATLAB simulator and the results of the proposed techniques are discussed, and in the end, the performance evaluation of the method is presented according to the intended scenarios. Eventually, Section 5 summarizes the results of the study.

2. Literature Review

In [23], a model-free scheme is introduced which is capable of identifying the topology changes in distribution networks using the data of phase measurement units at the distribution level (DPMU). In this work, algebraic tools of behavioral system theory are utilized to progress easy-to-implement algorithms and the inherent problems associated with the D-PMU measurement and their proposed solution are discussed as an additional challenge to implement the proposed algorithms.

Frequency disturbance events (FDEs) occur due to various events such as generator trip (GT), blackout line (LO), and load interruption (LD) that affect the stability of power systems. Depending on the intensity of the disorder, small properties strongly affect the performance of the integrated system. Accurate and rapid recognition of the event and its location in monitoring the adequacy of resources and

preventing the economic loss and extinction is very imperative. The article [24], by concentrating on an advanced online hierarchical process, first recognizes the event and then identifies its classification. Finally, the exact location of FDE is found based on PMUs data. Compared with other articles, which are focused only on the classification or location of events, both goals are generated using the proposed new hierarchical framework. This study utilizes the deep learning (DL) progress for developing a recurrent neural network (RNN) model and a long short-term memory (LSTM) model for detection and localization of FDE with considerable precision. In this research, only a few time series frequency change rates (ROCOF) received from a limited number of PMUs are used as input to the DL algorithm. This hierarchical method has been tested on New England 39-bus, IEEE 14 bus systems, and the modified IEEE 118-bus system. The assessment results indicate the potential application of the proposed models for the detection and classification of FDEs compared to conventional algorithms and the frequency-based DL model. The proposed models have accomplished significant classification accuracy [25].

An imperative subject for fault classification in power distribution systems is the restriction of fault data for training classifiers to recognize types of power outages for repair. Measuring data from power systems are generally not labeled without specific types of faults, and labeled data with very limited types of faults are very limited and challenge educational classifiers with sufficient accuracy. Present fault classification methods for dealing with labeled small samples ascertain the underlying structures between labeled and unlabeled data. However, this line of methods has incorrect assumptions about nonlabel and labeled data and suffers from loss of accuracy when dealing with limited data that have a tag. The paper [26] suggests a novel latent structure learning under a multitask learning framework to supplement the information and address the challenges of limited-tagged data for fault organization. The proposed process not only uses the underlying structure of unlabeled data that is not used effectually but also eliminates the boundaries of learning the underlying structure by avoiding classifiers from being equipped with unlabeled data.

Rapid and accurate localization of electrical faults along power grids increases the reliability and continuity of the source, the rapid recovery of the power supply, and the consequent reduction of downtime. The paper [27] presents a method of locating network fault through multidata source information fusion. The compressed sensing algorithm is used to reconstruct the electrical signal twice and the rough fault amplitude and the degree of fault are achieved, respectively. Then, to attain the degree of switching fault of each element in the anomalous fault range, the Bayesian network is used. Finally, the DS evidence theory combines these two degrees of fault to obtain the result of spatial location. In [28], a new technique for online fault location tracking in distribution networks based on existing systems measurement using phaser units (PMUs) and iterative support detection (ISD) is presented. Through the fault event and by default, voltages are measured by PMUs that are optimally located along the network. From the voltage change vector and the system impedance matrix, the flow change vector contains a nonzero element with the faulty part. Since PMUs are not located in all crossings, the system equation has already been determined. Hence, to solve a flow vector that has a rare nature, ISD method is utilized. The paper [29] considers the fault location algorithm suitable for medium unbalanced overhead distribution systems with or without distribution generation (DG). It should be noted that the proposed algorithm uses only simultaneous voltage measurement from two measurement points within the distribution system. Utilizing the basic fault analysis based on the bus matrix and the base impedance, objective algorithm estimates the fault position for each type of accurate short circuit fault. Fault resistance is considered in the algorithm, but it is not explicitly used in the transmission line impedance matrix.

To improve the sensitivity and reliability of system protection, detection, identification, and location are fundamental. This allows power systems to preserve stable performance. However, it is challenging in large-scale multidevice power systems. The authors in [30] present three new models of classification and deep learning regression (DL) based on deep neural networks (DNNs) for fault area identification (FRI), fault type classification (FTC), and fault location prediction (FLP). These new models ascertain transient data from pre- and postfault cycles for reliable decision making, while current and voltage signals are measured by phasor measurement units (PMU) at different terminals and are used as input features in DNN models. Here, sequential deep learning (SDL), through long short-term memory (LSTM) and high-dimensional multivariate features are utilized to model spatiotemporal series to accomplish accurate classification and prediction results.

Among the methods of fault localization, the most common of these methods is based on fundamental phase-based methods, whose approximation tends to converge with the stable state structure prior to opening the circuit breaker. Thus, conventional troubleshooters typically consider phase estimates obtained from shield relays or class P phase-measuring units, which show the time of filter delay less than the phasor measurement units of the class M. However, it is usually assumed that phasor measurement samples of M class are not suitable for fault location applications due to inherent filtering delays; studies on the possibility of using class M data-based fault locating programs are still scarcely found in literature [31]. The paper [32] was introduced to investigate whether the phasor measurement units of class M could be used in real location fault localization schemes using previously used measurement systems. In order to do so, the real fault events on the Brazilian electricity network are investigated and the performance of four different phasor measurement algorithms is assessed when phasor measurement models are used in a traditional protection relay algorithm and from the phasor measurement units of class M. As opposed to initial expectations, the obtained results indicate that the M-class phase measurements can be used in fault location applications because in the phase-based fault localization methods, faults are expected at the expected levels.

The authors in [33] present an approach that enables the fault location across the system using a small set of phase measurements. The proposed algorithm combines the prediction of voltage after fault and the scatter estimation. The obtained method allows for practical use of the scattering formula using Prony analysis to predict stable state voltages after faults at those buses equipped with phasor measurement units. A short transient recording is required for prediction only, which is usually accessible before the protective relays are activated. After the prediction stage, recognizing the location of the fault is essential from the least-angle scatter regression-based scattering estimation algorithm. However, for certain circumstances that are usually associated with small fault currents, the scattered estimate algorithm may not be able to accurately diagnose the location of the fault. To lessen this problem, ordinary least squares are used to increase the strength of the proposed method.

It is worthy to note that local protective elements such as fuses and relays are the first protection mechanism to overcome the fault and separation of the damaged portion of the power network. Although the capability of choice, speed, and sensitivity of these initial protective devices are relatively high and they cannot be considered flawless, there is small percentage of events for which the relays experience a fault occurrence. For these scenarios, a redundant arrangement can be made through backup protection. In [34], a centralized remote protection method based on two techniques, the Delta algorithm, and the least squares technique have been proposed. The proposed method identifies the transmission line, fault type, and distance to fault. Moreover, the phasor measurement unit data is utilized and is nonreproducible. According to phase measurement units, the network is divided into a number of subregions in order to accurately determine the location of the fault location. In the first stage, the affected area is located and then a deep search in the fault zone is carried out to determine the fault line. Ultimately, the fault distance is determined according to the distributed model of the transmission line.

In [35], a new high-voltage transmission line fault location scheme based on the use of support vector regression (SVR) has been proposed. The proposed scheme will only use the amplitude of the fault voltage wave amplitudes, measured at one end of the line. The various types of faults are investigated in different locations with different default impedance and types of fault initiation angles in the voltage transmission line of 400 kv and 300 km. Fault voltages are attained from the signals of the 1/8 cycle after the fault and also the removal of noise using a low-pass filter. The amplitude of the fault voltage signals is used as features for the SVR training. Subsequently, the SVR is used in the precise location of the fault on the transmission line. Compared to other fault locating schemes, the proposed scheme for estimating fault locations requires no information and a smaller data window. However, the proposed scheme gives more accurate estimates, regardless of fault types, fault initiation angles, and default impedance.

The paper [36] proposes a real-time fault detection technique and fault line detection capability obtained by calculating synchronous phase-based estimators. Each state estimator is characterized by different and reinforced topology in order to contain a floating fault bus. It should be noted that the choice of state estimator that affords the correct solution is made by a criterion that calculates the sum of the weighted residues. The proposed process design is validated using a real-time simulation platform in which an active flow distribution network with a PMU-based monitoring system is simulated. It is postulated that the proposed process for active and passive networks, with neutral ground connection and without neutral ground connection, is appropriate for low and high impedance faults of any kind (symmetric and asymmetric) that occur in different places.

The authors in [37] present an innovative method for fault localization in distribution networks based on the analysis of classical circuits. Two synchronized and few nonsynchronized pre- and during-fault voltages are required in few buses beside the impedance matrix. A new impedance matrix manipulation method is suggested to survey the distribution system in partitions under multiple subsystems. This method allows the fault localization process to be solved by solving the equations of equations that are determined and this method is technically available. This fault is determined by analyzing the voltage drop across the terminal-bus of each subsystem separately.

Owing to the presence of different branches in the electric distribution network and the only accessible information on voltage and current at the beginning of the line and the unavailability of information at the end of the network, the detection of fault section in the distribution network is very essential. Smart meters are now used to measure voltage and flow of network lines, but due to limitations of installation sites, it is not possible to use these devices in all network lines. In [38], two techniques have been used to ascertain the fault section and the fault occurrence location in the network to estimate the fault distance at the beginning of the line with the current estimation at the end of each network line. Therefore, in this project, by installing smart meters in the main branch of the network, as well as information obtained from the current in the normal state of the network, we have tried to practically estimate the voltage and current at the beginning and end of each distribution. The network line in this method uses more power flow to compute the voltage drop and voltage estimation of the voltage and current at the end of the network lines to determine the fault area.

3. Conception

In power distribution networks, for accurate positioning of fault, different network states must be considered in fault estimation. In this section, we try to define concepts that are addressed and devoted to this article. First, the types of faults studied in this work are modeled and investigated for two fault detection systems in the network with no distributed generation sources and the impact of fault on the network will be discussed.

3.1. Types of Faults (Considered in This Study). Basically, the faults that may occur in a distribution feeder are single-phase to ground faults with ground resistance R_f and two-phase faults to ground with R_{arc} arc resistance and ground resistors R_f in different phases, and three-phase connection faults to ground. Before presenting the fault locating

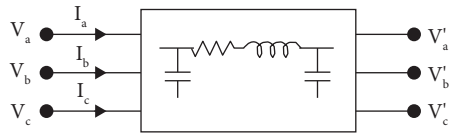

Figure 1: The circuit model of the branch division between the two buses.

algorithm, these three types of short circuit faults are modeled as shown in Figure 1.

3.1.1. Single-Phase to Ground-Fault Modeling. A single-phase short-to-ground fault with ground resistance R_f at distance d in terms of prionite from the node at the beginning of the fault section is shown in Figure 2. According to the figure, the relationship between the voltage at the beginning of the section and the location of the fault can be written as follows:

$$V_a = d.\left(z_{11}.I_a + z_{12}.I_b + z_{13}.I_c\right) + V_{fa}. \tag{1}$$

On the other hand, it can be written as follows:

$$V_{fa} = R_f.\left(I_a - \mathrm{I}'_{\mathrm{a}}\right). \tag{2}$$

The value of the current phasor, I'_a, is obtained by implementing the load distribution algorithm presented in [39] in the downstream distribution feeder of point f holding the V_{fa} voltage phasor. However, since the location of point f, i.e., distance d, is unknown, so with a good approximation, the downstream distribution feeder of point S can be loaded

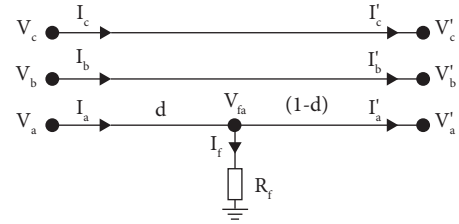

Figure 2: Single-phase fault circuit model.

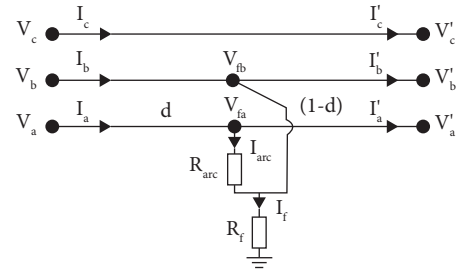

Figure 3: The circuit model of two-phase fault to each other and to ground.

without considering the fault with the existing voltage phase of V_a and the calculated current I_a instead of the current value I'_a used.

By substituting (2) in (1) and decomposing the result into two real and imaginary components, the values of R_f and d can be obtained; the value of d is given in the following relation:

$$d = \frac{\mathrm{Im}\left[\left(\mathrm{Re}\left(V_a\right) - \mathrm{j} * \mathrm{Im}\left(\mathrm{V_a}\right)\right) * \left(\mathrm{Re}\left(I_a - \mathrm{I}'_{\mathrm{a}}\right) + \mathrm{j} * \mathrm{Im}\left(I_a - \mathrm{I}'_{\mathrm{a}}\right)\right)\right]}{\mathrm{Im}\left[\left(\mathrm{Re}\left(z_{11}\,I_a + z_{12}\,I_b + z_{13}\,I_c\right) - \mathrm{j} * \mathrm{Im}\left(z_{11}\,\mathrm{I_a} + z_{12}\,\mathrm{I_b} + z_{13}\,\mathrm{I_c}\right)\right) * \left(\mathrm{Re}\left(I_a - \mathrm{I}'_{\mathrm{a}}\right) + \mathrm{j} * \mathrm{Im}\left(I_a - \mathrm{I}'_{\mathrm{a}}\right)\right)\right]}. \tag{3}$$

3.1.2. Modeling Two-Phase Fault to Each Other and to Ground. In this case, a two-phase fault to each other and to ground occurred at a distance d from the beginning of the fault section with R_{arc} arc resistance and ground resistance R_f, which is shown in Figure 3. As in the previous case, based on equation (1), the voltage of the faulty phases at the beginning of the desired section and the fault location can be written as the following equations:

$$\begin{aligned} V_a &= d.\left(z_{11}.I_a + z_{12}.I_b + z_{13}.I_c\right) + V_{fa}, \\ V_b &= d.\left(z_{21}.I_a + z_{22}.I_b + z_{23}.I_c\right) + V_{fb}. \end{aligned} \tag{4}$$

Regarding the aforementioned relations, the following relations are presented:

$$\begin{aligned} V_a - V_b = d\,&\left[\left(z_{11} - z_{21}\right)I_a + \left(z_{12} - z_{22}\right)I_b\right. \\ &\left. + \left(z_{13} - z_{23}\right)I_c\right] + \left(V_{fa} - V_{fb}\right). \end{aligned} \tag{5}$$

On the other hand, it can be written according to Figure 3:

$$V_{fa} - \mathrm{V_{fb}} = \mathrm{R_{arc}}.\left(\mathrm{I_a} - \mathrm{I}'_{\mathrm{a}}\right). \tag{6}$$

By substituting (6) in (5), the values of R_f and d can be obtained as in the single-phase ground mode, with the fault distance d:

$$d = \frac{\mathrm{Im}\left[\left(\mathrm{Re}\left(V_a - V_b\right) - \mathrm{j} * \mathrm{Im}\left(\mathrm{V_a} - \mathrm{V_b}\right)\right) * \left(\mathrm{Re}\left(I_a - \mathrm{I}'_{\mathrm{a}}\right) + \mathrm{j} * \mathrm{Im}\left(I_a - \mathrm{I}'_{\mathrm{a}}\right)\right)\right]}{\mathrm{Im}\left[\left(\mathrm{Re}\left(\left(z_{11} - z_{21}\right)I_a + \left(z_{12} - z_{22}\right)I_b + \left(z_{13} - z_{23}\right)I_c\right) - \mathrm{j} * \mathrm{Im}\left(\left(z_{11} - z_{21}\right)\mathrm{I_a} + \left(z_{12} - z_{22}\right)\mathrm{I_b} + \left(z_{13} - z_{23}\right)\mathrm{I_c}\right)\right) * \left(\mathrm{Re}\left(I_a - \mathrm{I}'_{\mathrm{a}}\right) + \mathrm{j} * \mathrm{Im}\left(I_a - \mathrm{I}'_{\mathrm{a}}\right)\right)\right]}. \tag{7}$$

3.2. Fault Locating in the Distribution Network. In the first part, the fault location in the distribution network can be discussed without the presence of production sources and in the second part of the fault location in the distribution network with the presence of distributed generation sources. The fault of connecting three phases to ground is described here.

3.2.1. Fault Finding without the Presence of Distributed Generation Sources. The distribution network consists of all different branches. Branch is a part of the distribution network between two successive buses and there is only one line between which there is no other element. The single-line view of each section is shown in Figure 4(a). In this part, the π line model has been used for accurate modeling of each part. Therefore, the circuit model of each section can be extracted as shown in Figure 4(b).

To determine the fault distance according to the π model, the voltage line of point n at distance l from equation (8) is calculated [35].

$$\begin{bmatrix} V_{R\,\mathrm{abcn}} \\ I_{R\,\mathrm{abcn}} \end{bmatrix} = \begin{bmatrix} a_l & -b_l \\ -c_l & d_l \end{bmatrix} \begin{bmatrix} V_{S\,\mathrm{abcm}} \\ I_{S\,\mathrm{abcm}} \end{bmatrix}. \tag{8}$$

The coefficients a, b, c, and d are calculated from the following equations [21]:

$$\begin{aligned} a_l &= d_l = I + 0.5 \times Z_{\mathrm{ABC}} \times Y_{\mathrm{ABC}} \times I^2, \\ b_l &= Z_{\mathrm{ABC}} \times I, \\ c_l &= Y_{\mathrm{ABC}} \times I + 0.25 \times Y_{\mathrm{ABC}} \times Z_{\mathrm{ABC}} \times Y_{\mathrm{ABC}} \times I^3, \end{aligned} \tag{9}$$

$V_{S\,\mathrm{abc}}$: voltage at the beginning of the line
$I_{S\,\mathrm{abc}}$: the current at the beginning of the line
Z_{ABC}: line impedance matrix
Y_{ABC}: the admittance matrix or capacitance of the line
$V_{R\,\mathrm{abc}}$: voltage at the end of the line
$I_{R\,\mathrm{abc}}$: the current at the end of a line
I: identity matrix

$$V_{R\,\mathrm{abcn}} = a_1 \times V_{S\,\mathrm{abcm}} - b_1 \times I_{S\,\mathrm{abcm}}, \tag{10}$$

$$I_{R\,\mathrm{abcn}} = -c_1 \times V_{S\,\mathrm{abcm}} + d_1 \times I_{S\,\mathrm{abcm}}. \tag{11}$$

Figures 5(a) and 5(b) show the single-line view and circuit model of a part of the distribution network when a fault occurs.

According to Figure 5(a), if fault occurs at location F, it can be observed. Hence, this can be created in the model line block π, before the fault point and after the fault point. When fault occurs at location F, the fault point voltage at distance x from the beginning of the branch is calculated with the following relation:

$$V_F = d_x \times V_S - \mathrm{b_X} \times \mathrm{I_S}. \tag{12}$$

Figure 6 shows the general model of the fault.

According to Figure 6, the fault-point voltage matrix is defined as follows:

$$\begin{bmatrix} V_{Fa} \\ V_{Fb} \\ V_{Fc} \end{bmatrix} = \begin{bmatrix} Z_{Fa} + Z_{Fg} & Z_{Fb} & Z_{Fc} \\ Z_{Fa} & Z_{Fb} + Z_{Fg} & Z_{Fc} \\ Z_{Fa} & Z_{Fb} & Z_{Fc} - Z_{Fg}. \end{bmatrix} \begin{bmatrix} I_{Fa} \\ I_{Fb} \\ I_{Fc} \end{bmatrix}. \tag{13}$$

The fault phase has an opposite current of zero, so equation (13) in phase k is given equal to equation (12) and (14) results.

$$Z_{FK}.I_{FK} + Z_{Fg}.I_{Fg} = V_{SK} + x^2.\,0.5.\,M_K - x.N_K, \tag{14}$$

where I_F includes the sum of the fault currents in all phases.

$$\begin{bmatrix} M_a \\ M_b \\ M_c \end{bmatrix} = \begin{bmatrix} Z_{aa} & Z_{ab} & Z_{ac} \\ Z_{ba} & Z_{bb} & Z_{bc} \\ Z_{ca} & Z_{cb} & Z_{cc} \end{bmatrix} \begin{bmatrix} Y_{aa} & Y_{ab} & Y_{ac} \\ Y_{ba} & Y_{bb} & Y_{bc} \\ Y_{ca} & Y_{cb} & Y_{cc} \end{bmatrix} \begin{bmatrix} V_{Sa} \\ V_{Sb} \\ V_{Sc} \end{bmatrix}, \begin{bmatrix} N_a \\ N_b \\ N_c \end{bmatrix} = \begin{bmatrix} Z_{aa} & Z_{ab} & Z_{ac} \\ Z_{ba} & Z_{bb} & Z_{bc} \\ Z_{ca} & Z_{cb} & Z_{cc} \end{bmatrix} \begin{bmatrix} I_{Sa} \\ I_{Sb} \\ I_{Sc} \end{bmatrix}. \tag{15}$$

It should be noted that the results are from n equations where n represents the total number of fault phases. By dividing relation (14) into two parts, real and imaginary, and considering the pure resistance of Z_{Fa}, Z_{Fg} and Z_{Fc}, Z_{Fb}, respectively, the results are obtained:

$$\begin{aligned} &R_{Fk}.I_{Fkr} + R_{Fg}.I_{Fkr} - \mathrm{x_{Fg}}.\mathrm{I_{Fki}} \\ &\quad = V_{Sk} + x^2.\,0.5 \times M_{kr} - N_{kr} = T_{kr}, \end{aligned} \tag{16}$$

$$\begin{aligned} &R_{Fk}.I_{Fki} + R_{Fg}.I_{Fki} - \mathrm{x_{Fg}}.\mathrm{I_{Fki}} \\ &\quad = V_{Sk} + x^2.\,0.5 \times M_{ki} - N_{ki} = T_{ki}, \end{aligned} \tag{17}$$

where r represents the real part and i represents the imaginary part and is obtained by removing R_{Fk} from equations (16), (17), and (18). Im is the imaginary part and Re is the real part.

$$\begin{aligned} &R_{Fg}.\mathrm{Im}\left[I_{Fk}.I_F^*\right] - X_{Fg}.\mathrm{Re}\left[I_{Fk}.I_F^*\right] \\ &\quad + \left[T_{kr}.I_{Fki} - T_{ki}.I_{Fkr}\right] = 0, \end{aligned} \tag{18}$$

$$\begin{aligned} &R_{Fg}.\mathrm{Im}\left[I_F.I_F^*\right] - X_{Fg}.\mathrm{Re}\left[I_F.I_F^*\right] \\ &\quad + \sum_{\mathrm{k}=\Omega\mathrm{k}} \left[T_{kr}.I_{Fki} - T_{ki}.I_{Fkr}\right] = 0. \end{aligned} \tag{19}$$

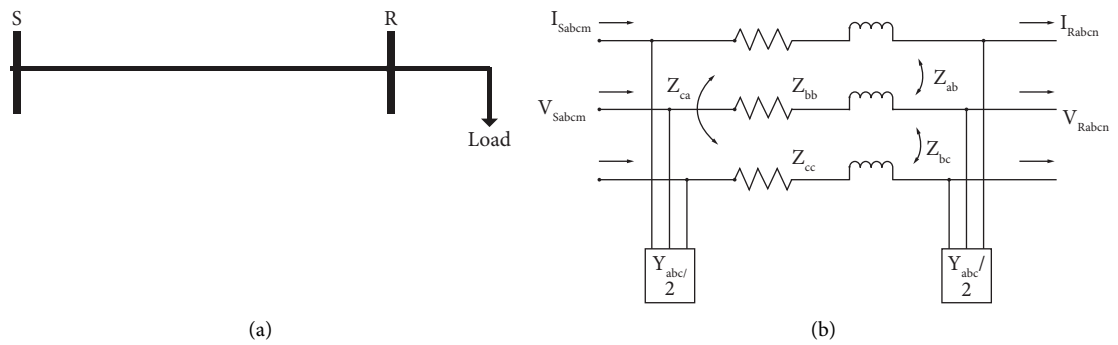

Figure 4: (a) Single line view of each part of the distribution network. (b) Circuit view of each part of the distribution network.

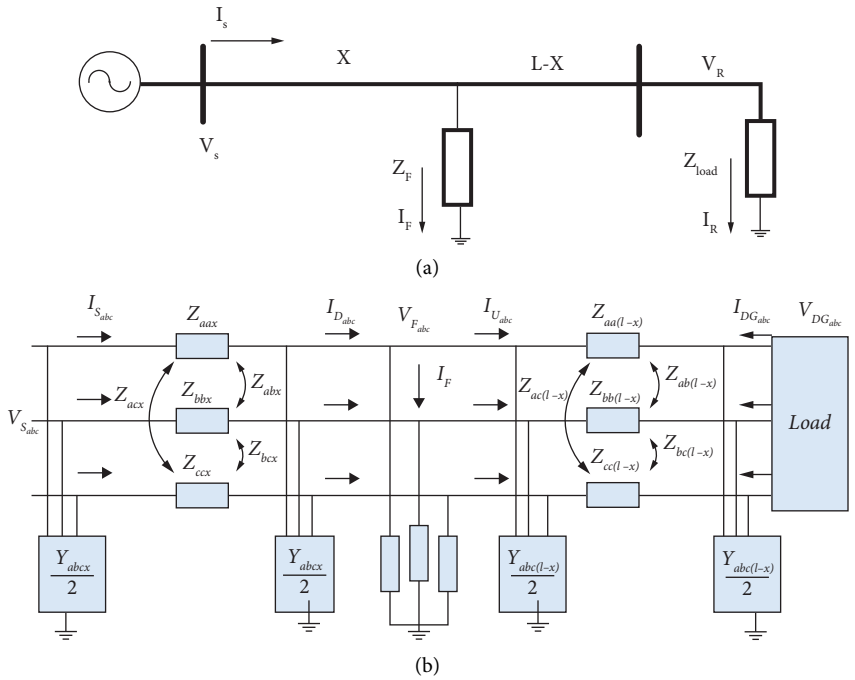

Figure 5: (a) Single line view of each part of the distribution network. (b) Circuit view of each part of the distribution network when fault occurs.

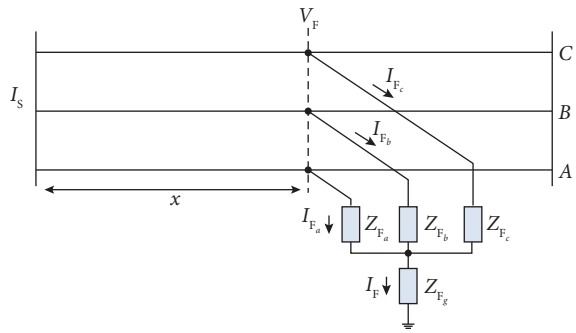

Figure 6: General view of resistance fault.

Given that the multiplication of two complex numbers in one's conjugate is equal to a real number and its imaginary part is zero, as well as the faults in the resistive power system, equation (14) has been rewritten from equations (11) and (12).

$$\begin{aligned} \mathrm{Im}\left[I_F.I_F^*\right] &= \mathrm{Im}\left\{\left|I_F\right|^2\right\} = 0, \\ \sum_{k\in\Omega k}\left[T_{kr}.I_{Fki} - T_{ki}.I_{Fkr}\right] &= 0, \end{aligned} \tag{20}$$

$$\begin{aligned} x^2\left[0.5\sum_{k\in\Omega k} Im\{M_k.I_{Fk}^*\}\right] - x\left[\sum_{k\in\Omega k} Im\{N_k.I_{Fk}^*\}\right] \\ + \left[\sum_{k\in\Omega k} Im\{M_{Sk}.I_{Fk}^*\}\right] = 0. \end{aligned} \tag{21}$$

In general, equation (21) can be rewritten according to

$$\begin{aligned} a_2\times x^2 + a_1\times x + a_0 &= 0, \\ \Delta &= a_1 - 4\times a_2\times a_0. \end{aligned} \tag{22}$$

So,

$$x_1 = \frac{\left(-a_1 \pm \sqrt{\Delta}\right)}{2\times a_2}. \tag{23}$$

3.2.2. Fault Location in the Distribution Network with the Presence of Distributed Generation Sources. To determine the fault distance in this section, an algorithm is first implemented for one section and this algorithm is generalized to more sections. Having the voltage and current at the beginning of the feeder and the voltage and current at the end of the feeder, which is the same voltage and current towards the distributed sources, the fault distance π is determined using the impedance algorithm based on the π model. Figure 7 shows a single-line view and circuit model of a distribution feeder with the presence of distributed generation sources.

Now, suppose fault occurs in the system. Figure 8 shows the error in the system. Fault point voltage is displayed with V_f. The fault point voltage is obtained by using the source voltage and the line model matrix π line, or by using the distributed source voltage, or, in other words, the line end voltage and the line matrix π model. The fault point voltage is equal from the source side and from the distributed generation sources.

Assume that the fault point voltage is calculated according to equation (8) by the source at distance x from

$$V_{Fs} = V_S + 0.5\times zz\times Y\times V_S\times x^2 - zz\times x\times I_S. \tag{24}$$

The voltage of the fault point is calculated from equation (25) from the distributed generation sources that is located at the $l - x$ distance.

$$\begin{aligned} V_{\mathrm{FDG}} = V_{\mathrm{SDG}} &+ 0.5\times zz\times Y\times V_{\mathrm{SDG}} \\ &\times (l-x)^2 - zz\times(l-x)\times I_{\mathrm{SDG}}. \end{aligned} \tag{25}$$

The fault voltage from the distributed generation sources is set equal to the fault voltage from the source. A quadratic equation gives the following results:

$$\begin{aligned} 0.5\times zz\times Y\times\left(V_S - V_{DG}\right)\times x^2 &+ Y\times zz\times l\times V_{DG} \\ - zz\times l\times V_{DG} & \\ - zz\times\left(I_S - I_{DG}\right)\times x &+ V_S - V_{DG} \\ - 0.5\times l^2\times zz\times l\times I_{DG} &= 0. \end{aligned} \tag{26}$$

In general, equation (26) can be rewritten according to

$$\begin{aligned} a_2\times x^2 + a_1\times x + a_0 &= 0, \\ \Delta &= a_1 - 4\times a_2\times a_0. \end{aligned} \tag{27}$$

So,

$$x_1 = \frac{\left(-a_1 \pm \sqrt{\Delta}\right)}{2\times a_2}. \tag{28}$$

3.3. Genetic Algorithm (GA). Genetic algorithm is a computational model that solves optimization problems by imitating genetic processes and evolution theory [40, 41]. Solutions of a population set are used to form a new population set. This is hoped that the new population will be better than the previous population. The solutions that make new solutions are chosen according to their fitness: the more appropriate they are, the more likely they are for reproduction. This is repeated until some conditions (e.g., a number of generations or improvement in the best solution) are met. In traditional GA, all variables of interest must first be encoded as binary digits (genes) of a string (chromosome). To minimize a function $f(x_1, x_2, \ldots, x_k)$ using GA, each x_i is first encoded as a dual or floating string of length m. Thus,

$$\begin{aligned} X_1 &= [11110, \ldots, 01011], \\ X_2 &= [00101, \ldots, 11110], \\ X_k &= [10001, \ldots, 01001], \end{aligned} \tag{29}$$

where $\{x_1, x_2, \ldots\ldots, x_k\}$ is called a chromosome and x_i is a gene. Then, three standard genetic operations, namely, reproduction, crossover, and mutation, are accomplished to produce the new generation [42, 43]. Such procedures are repeated until the number of predetermined generations can be achieved or accurately required. The results are illustrated by chromosomes and the methods are known as the fitness function. The evolution of the GAs is shown in Figure 9, while the original methods are introduced with three main definitions.

Selection: the process in which solutions must be maintained or entitled to disappear or be selected (or authorized solutions). The best solution is selected and others are eliminated. Here, the fitness function and the optimization are quantitatively determined.

Crossover: a new solution is created from existing solutions after the selection process.

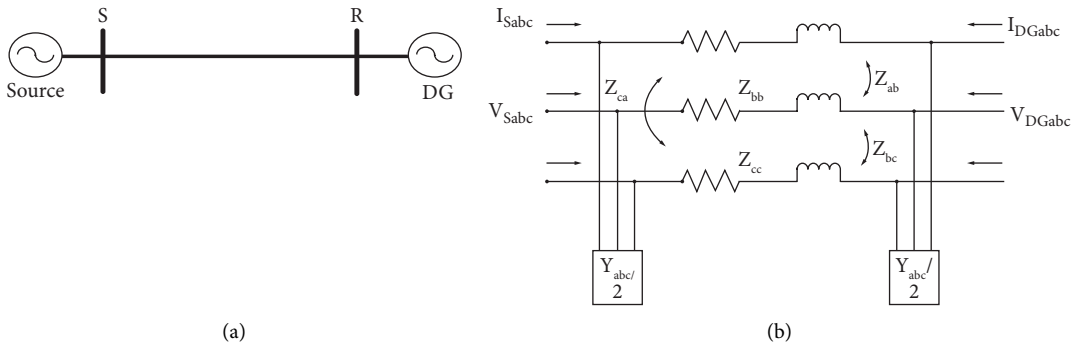

Figure 7: (a) Single-line view of a distribution feeder with distributed generation sources. (b) Circuit view of a distribution feeder with distributed generation sources.

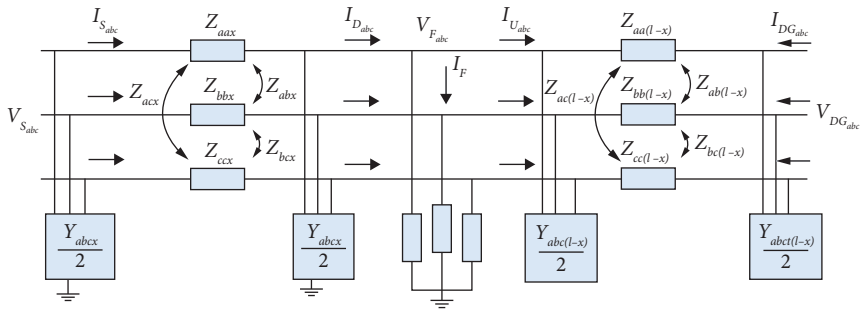

Figure 8: Incidence of errors in the distribution feeder with distributed generation sources.

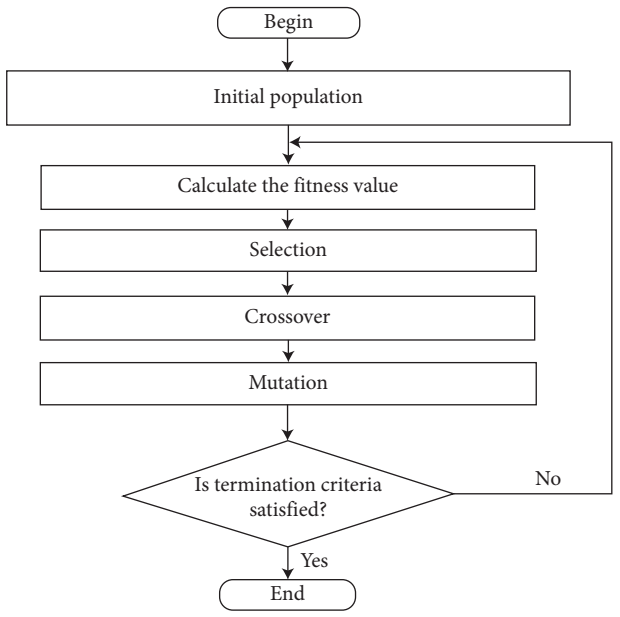

Figure 9: Flowchart of the standard genetic algorithm (GA) [41].

Mutation is the occasional introduction of new features into a solution string of the population. Mutation happens to preserve diversity within the population and prevent premature convergence.

3.4. Fuzzy Logic and Adaptive Neural-Fuzzy Inference System (ANFIS). Fuzzy logic is defined as a type of artificial methods used in the classification of fuzzy logic resource classification. Fuzzy logic theory is unclear in the scope of its activities or observations. In fact, fuzzy sets are developed, but it contains certain types of activities, such as "true-false" or numeric "1-0." Fuzzy logic is known for its simplicity and ease in the design of the algorithm, but when increasing the complexity of the system, you have difficulty to determine the appropriate set of rules and functions. In general, fuzzy rules and membership function are based on the behavior of the method learned by the neural network using input and output data [44]. Figure 10 shows an example of the membership functions created by the fuzzy rule generator.

In this study, the use of ANFIS is introduced. ANFIS is the intersection of an artificial neural network (ANN) and a fuzzy logic inference system. An artificial neural network is designed to mimic features of the human brain and includes a set of artificial neural cells. An adaptive system is a multilayer system in which each node (neuron) plays the capacity of the input signals. You can read more about the structure of ANFIS in [45–47]. Figure 11 shows a general diagram of the structure of ANFIS. In this figure, fixed nodes with a circle and adaptive nodes with a square are shown. The ANFIS technique uses the Sugeno fuzzy model [49], in which the fuzzy rules (if-then) are formulated by

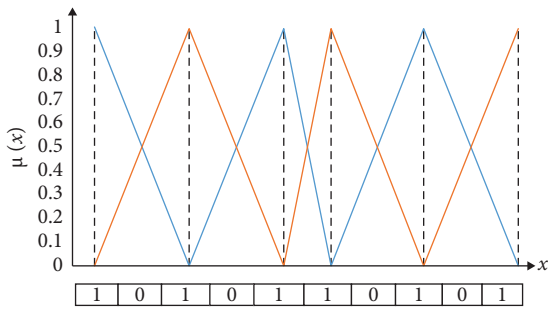

Figure 10: Membership function of fuzzy logic.

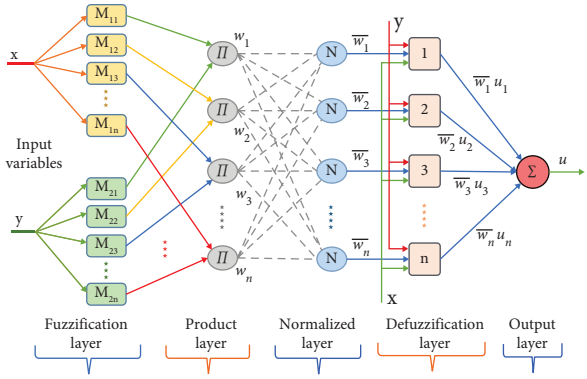

Figure 11: Schematic diagram of adaptive neuro-fuzzy inference system (ANFIS) architecture [48].

$$R_n\&9; = if\ M_{1i}(x)\, M_{2i}(y), \text{then } f \\ \&9; = p_n x(t) + q_n y(t) + r_n, \tag{30}$$

where n represents the number of rules. Note that M_{1i} and M_{2i} represent fuzzy membership functions. p_n, q_n, and r_n represent the linear parts of the corresponding n law.

Note that the first layer of ANFIS contains the initial fuzzification in which the degree of membership functions is represented using the input variable. Typically, each node in the layer represents an adaptive function formulated by [50]

$$M_{1i}\frac{1}{1+\left[X-c_i/a_i\right]^{b_i}}, \tag{31}$$

where (a_i, b_i, c_i) represent the set of parameters. Note that layer 2 stands for the product inference layer in which each node called P is controlled by a specific fuzzy rule. Note that the w_i output of the layer is displayed as follows:

$$w_i = M_{1i}(e) \times M_{2i}(\Delta e). \tag{32}$$

In turn, the third layer shows a normalization layer, while the transfer power calculated from the previous layer is normalized:

$$\overline{w_i} = \frac{w_i}{\sum_i (w_i)}. \tag{33}$$

Layer 4 receives the normalized values from the third layer. Note that each node in this layer represents a defuzzification mode with the node function as follows [51, 52]:

$$\overline{w_i}u = \overline{w_i}\left(P_i e + q_i \Delta e + r_i\right), \tag{34}$$

where (p, q, r), the result parameter, is set when u represents the control signal passed. Note that in the last layer, you have to calculate the sum of all the internal signals to collect the output of the rules [48]:

$$\sum_i (\overline{w_i}u) = \frac{\sum_i w_i u}{\sum_i w_i}. \tag{35}$$

4. The Proposed Method

Here, we describe our proposed process for detecting and locating faults in a default power distribution network. Regarding the studied faults, three models of single-phase, two-phase, and three-phase are studied, which can be generalized to other types of faults and only pay attention to ground connection faults. According to theoretical studies, as observed, the fault location estimation contains many complications and, on the other hand, the availability of branch flow or sections is critical and the problem of computation in different branches will require a series of computational complexity. This is while the voltage calculation at the feeder is independent of the path and the graph in the distribution network. Here, we focus our attention on the calculation of the error distance with the help of the voltage phasor measurement and not the calculation of the branch flow in the distribution network. In the proposed technique, we need only the amount of voltage phasor in the buses. Based on this, in a single network studied at a point of a unit D, PMU feeder is responsible for measuring the total voltages and is measured at any moment of time. The basis of our work in this paper is to calculate the voltage drop in each feeder when the error occurs when the fault occurs. It is also based on the proposed scheme to identify fault location after 0.1 s. Figure 12 shows the flowchart of the proposed scheme.

In this scheme, the phasor measurement voltage of each bus is checked regularly, and then the moment of the fault occurrence is detected by sudden voltage drop, which is determined in the next stage; according to the effective voltage drop in each phase, the type of ground connection fault of one, two, and three phases is determined and we enter the next stage. In this section, the difference between the voltage drop of each bus and the bus on the other side of each branch is calculated and aggregated for 0.1 seconds. Nodes with a more severe voltage drop are introduced, respectively, and any bus with a higher voltage drop is identified as a node subject to fault. Therefore, the fault must be calculated in the branches close to it. In the following, the calculated values of the difference in voltage drop of the branch are given to the fault positioning systems. In addition, information including line length and line length impedance according to model π is extracted for the fault event branch and this information is given to the fault location estimation system. In the last phase, the fault location estimation system analyzes these data factors and informs the operator the exact location of fault.

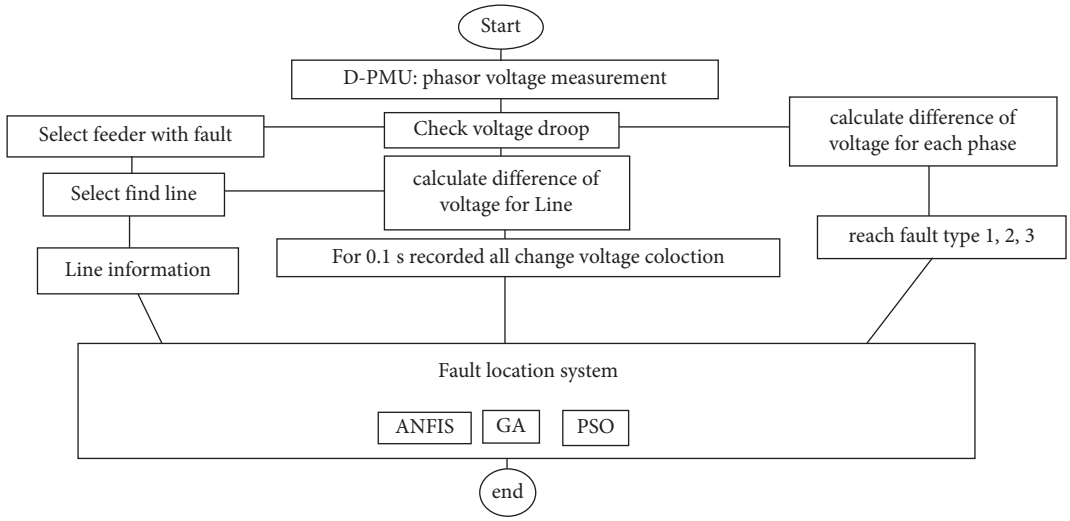

Figure 12: proposed flowchart.

4.1. Fault Location Estimation System along the Line. In this paper, we use three techniques to estimate the location of the fault along the line. The test data are extracted to investigate the faults and their information. Then, using a nonlinear model, we choose the location of the faults with the help of fuzzy neural methods, particle swarm optimization, and genetic algorithm. We have achieved an optimal model for estimating fault location in different types in the ANFIS method. In the following techniques, a nonlinear model of the third-order Taylor expansion is used, and we use the squares of the difference between the values of the nonlinear function and the real value as the objective function to determine the coefficients of the third-order nonlinear model, expressed in equation (36). With the help of the algorithms described above, these optimal coefficients are calculated:

$$\begin{aligned} &\text{function } z = \text{fitnessfunction } (x, y), \\ &\quad z = \text{sum}\,(\text{abs}\,((x(1) * y(:1).\hat{3} \\ &\qquad + x(2) * y(:1).\hat{2} + x(3) * y(:1) \\ &\qquad + x(4)).\hat{2} - y(:2).\hat{2})); \text{ end.} \end{aligned} \tag{36}$$

The target variables in this system are x_1, x_2, x_3, and x_4, which are defined as nonlinear models according to the input and output variables y_1 and y_2.

5. Simulation Results

In this section, the performance results of the proposed design based on three methods of location estimation including fuzzy neural network and nonlinear model optimized with genetic algorithm and particle swarm algorithm are reviewed and compared. In this work, the 9 bus network studied is shown in Figure 13. Information about each line in the network is collected and uploaded under MATLAB software. In this case, when for a grid defined in terms of the length and connections and impedance of the lines, the proposed systems are trained for the next steps for detection and test data, it works completely fast and in real time. The specifications of the computer used in this work are Intel Core i5 M480 @ 2.67 GHz.

Figure 14 illustrates the voltage drop for the error event in a branch between the 7 and 8 buses and displays the impact of this single phase error on the voltage drop at the different buses. The 25 km line has the highest voltage drop on the 7 and 8 bus. In Table 1, different fault cases have been investigated and selected, and for different fault lengths, it has been determined as the first option. According to Figure 14, the amount of voltage drop is different for different types of faults and the type of fault can be determined with a demarcation.

Figures 15–17 show the results of estimating the fault position with ANFIS, GA, and PSO methods, respectively, based on the comparison of actual and estimated results, and Table 2 shows the average fault percentage of the performance of all three methods. Based on the reviewed results, ANFIS method has provided more accurate results.

According to Table 1, for the types of faults taught to the estimator systems, in the first step, the location of the fault bus is identified, and in the second step, the exact position of the error is identified. First, the phasor voltage of each bus is regularly checked, and then the moment of the fault is detected by the sudden voltage drop. In this part, the amount of difference between the voltage drop of each bus and the bus on the other side of each branch is calculated, and according to the order of priority in the voltage drop that occurred in the buses, the locations of the buses with the most voltage drop are prioritized according to Table 1. In the next step, according to the effective voltage drop in each phase, the grounding fault type of one, two, and three phases is determined and we enter the next step. The first and second priority busses with the middle branch are prone to errors. Therefore, the error should be calculated in the branches close to it. In the following, the calculated values of the voltage drop difference of the branch are given to the fault location systems, along with that, the information including line length and line length impedance is extracted

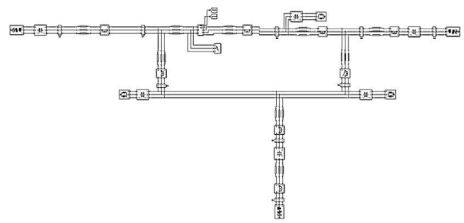

Figure 13: View the 9 bus distribution network under study.

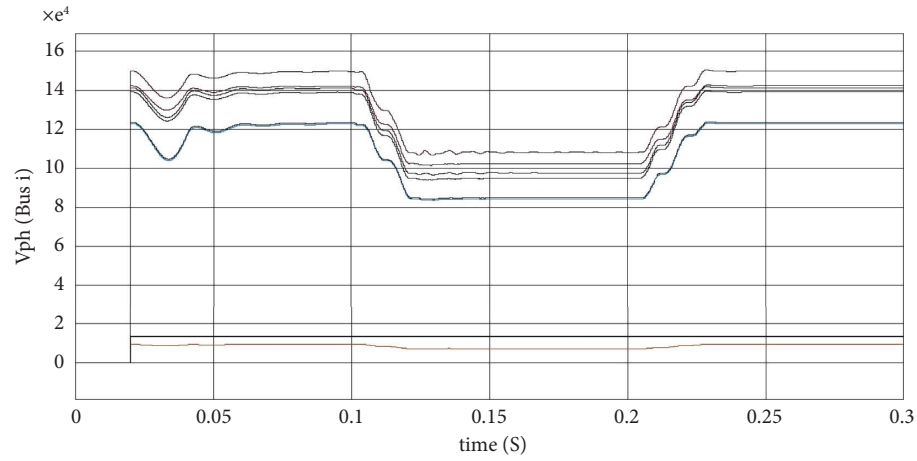

(a)

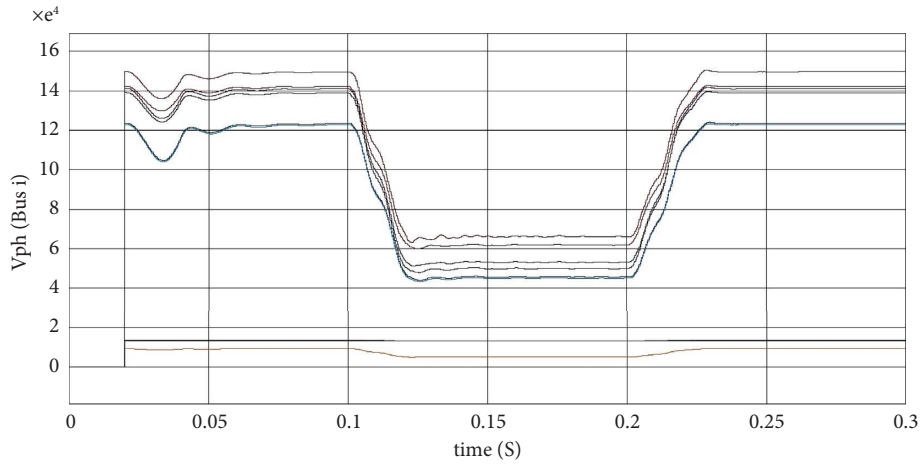

(b)

Figure 14: Continued.

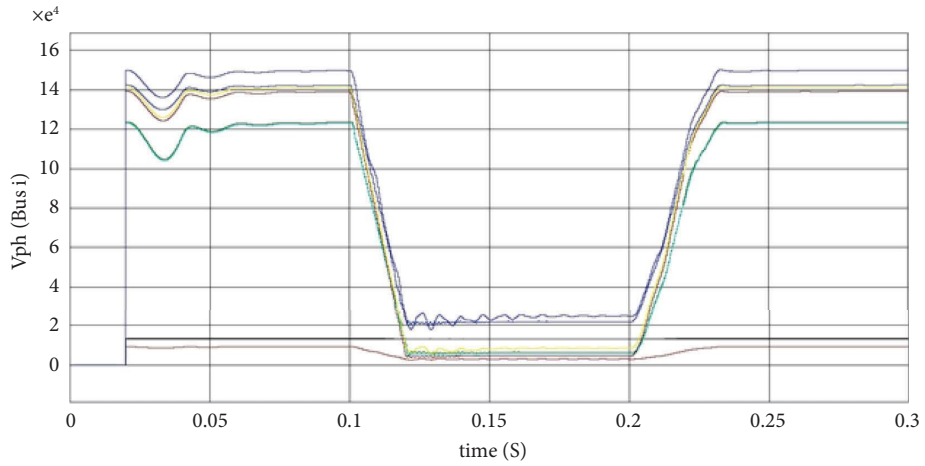

Figure 14: Display voltage drop for fault occurrence at a distance of 25 km. (a) Single-phase fault, (b) two-phase to ground, and (c) three-phase to ground.

Table 1: Display fault busses at different lengths.

Types of fault	1	1	2	2	3	3
Bus first priority	7	8	7	8	7	8
Bus second priority	8	9	8	9	8	9
Bus third priority	9	7	9	7	9	7
Distance	25	60	25	60	25	60

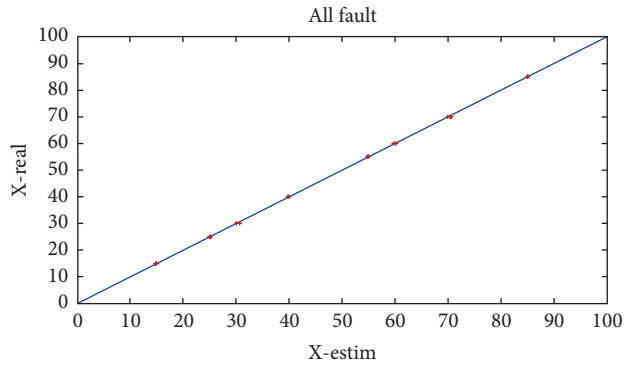

Figure 15: Adaptive neural fuzzy network fault length estimation system.

according to the π model for the same branch where the fault occurred, and this information is given to the fault location estimation system to be. In the last step, the fault location estimation system checks these information factors and informs the operator of the exact distance of the fault from the bus with the first priority. Table 2 shows the possible error in distance estimation for different proposed methods. This means the estimated distance for grounding event with this amount of distance estimation tolerance.

According to Table 2, neural fuzzy methods and GA genetic algorithms and PSO particle swarm have been used as different and comparative techniques to estimate the location and distance of different errors. Among these, the ANFIS neural fuzzy method has been able to identify the

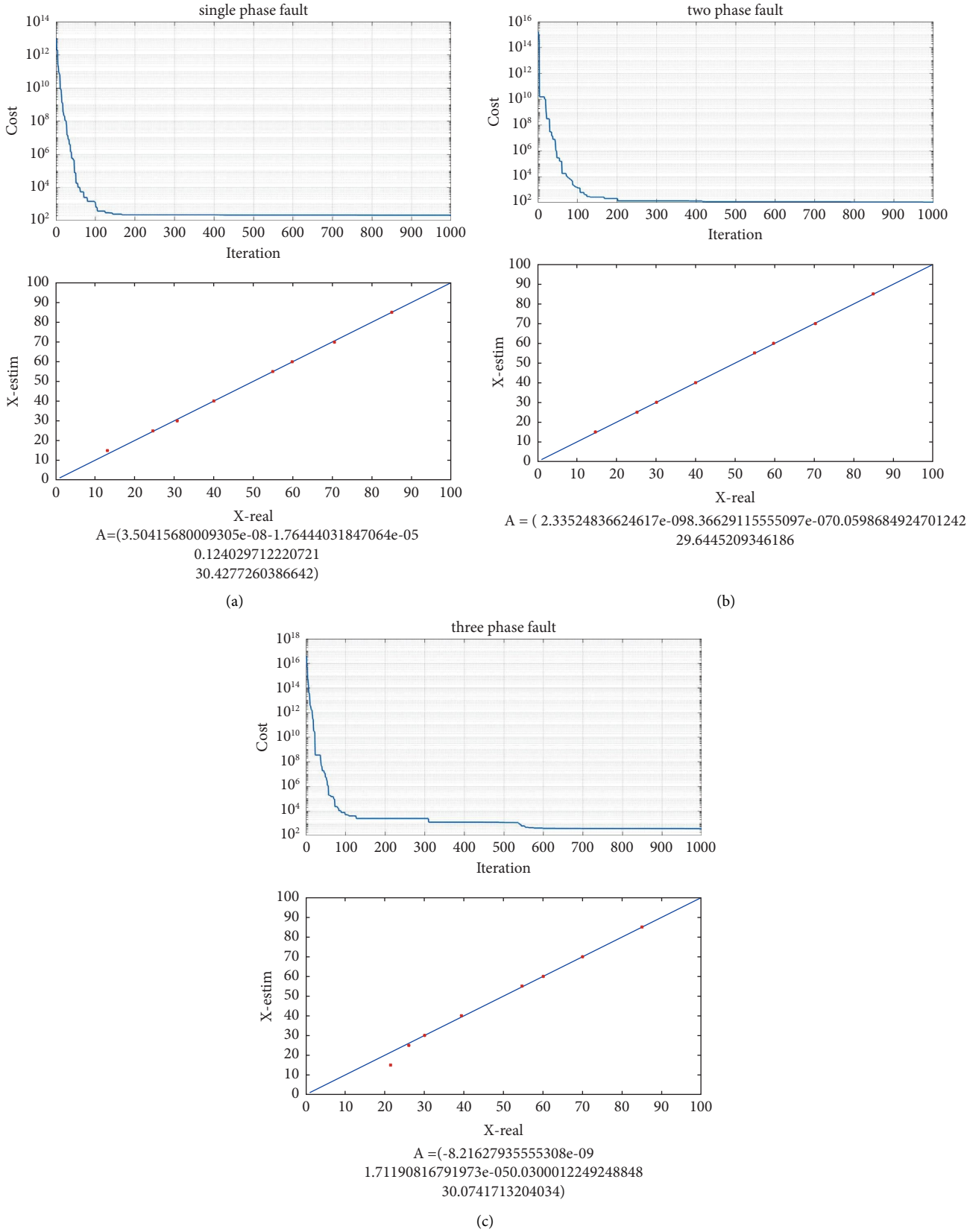

FIGURE 16: Nonlinear length estimation system optimized by genetic algorithm. (a) Single phase, (b) two-phase fault to ground, and (c) three-phase fault to ground.

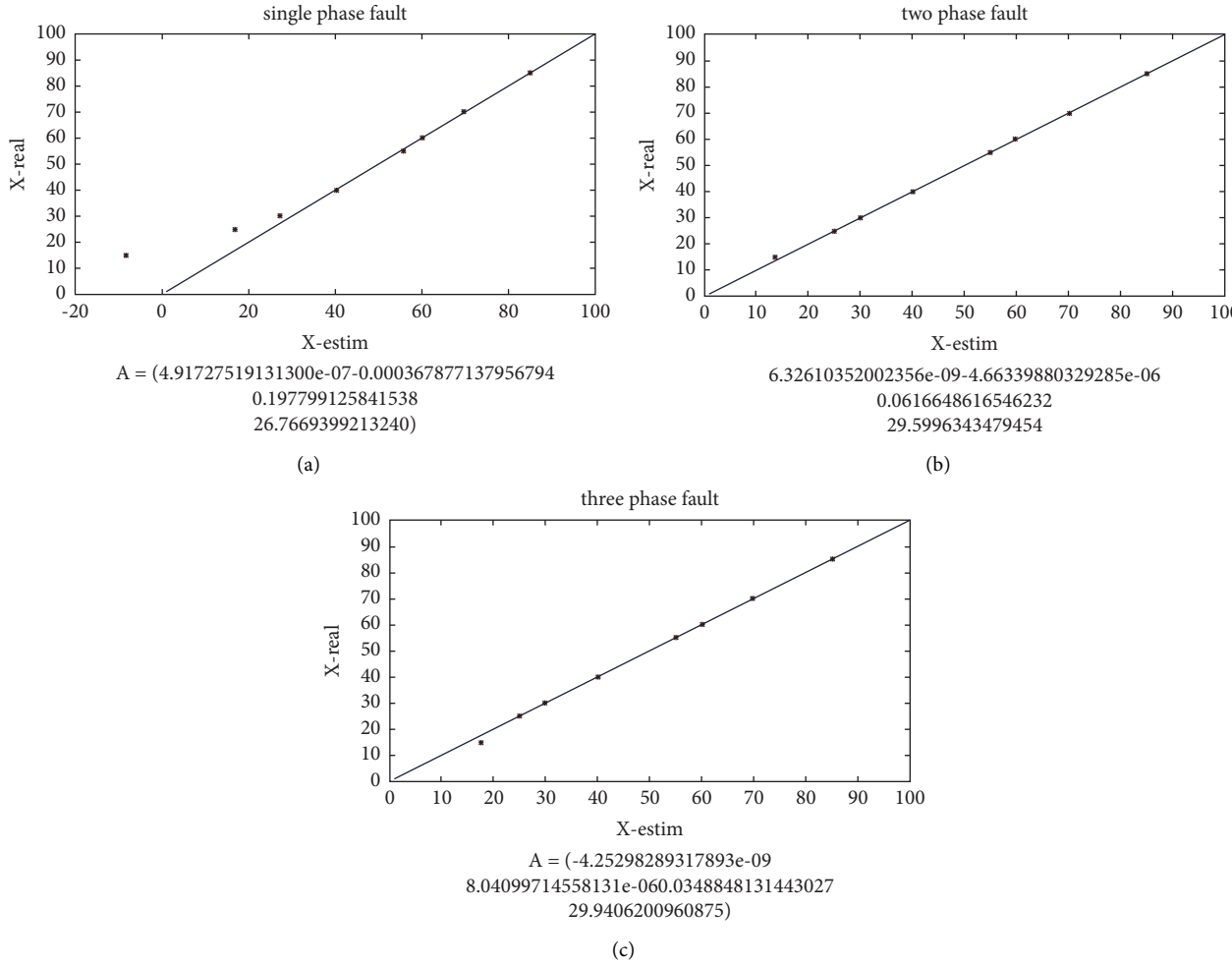

Figure 17: Nonlinear fault length estimation system optimized by particle swarm algorithm. (a) Single phase, (b) two-phase fault to ground, and (c) three-phase fault to ground.

Table 2: Comparison of the accuracy of the proposed estimating systems.

Proposed techniques	ANFIS	GA	PSO
Fault percentage for test samples (%)	0.34	2.54	6.3

exact location of the earth connection fault with the highest accuracy and lowest error tolerance.

6. Conclusion

Due to the increasing use of distributed generation sources in distribution networks, new proposed methods for finding fault in distribution network were provided by the presence of distributed generation sources to determine the fault location using the voltage information recorded at the beginning and end of the feeder and the distributed generation source. Due to the extent of distribution networks and the existence of multiple branches, fault locating in distribution networks is complicated into two parts: fault spacing in the distribution network without the presence of distributed generation sources and fault spacing in the distribution network with the presence of distributed generation sources. In this paper, the fault location was performed using a nonlinear quadratic equation model optimized with GA and PSO algorithms and the ANFIS neural fuzzy intelligent model without the presence of distributed generation sources in the distribution network with the presence of distributed generation sources using circuit relationships. The proposed methods were placed in different conditions such as single-phase, two-phase, and three-phase ground connection faults in different locations in the 9-bus network, and the results show the high accuracy of the proposed methods. Among these, the ANFIS method has shown better performance for correct fault locating.

Data Availability

The data used to support the study are available from the corresponding author upon request.

Conflicts of Interest

The authors declare that they have no conflicts of interest.

References

[1] M. M. Saha, J. Izykowski, and E. Rosolowski, *Fault location on power networks*, Springer, Berlin, Germany, 2010.

[2] S. Das, S. Santoso, A. Gaikwad, and M. Patel, "Impedance-based fault location in transmission networks: theory and application," *IEEE Access*, vol. 2, pp. 537–557, 2014.

[3] H. Fathabadi, "Novel filter based ANN approach for short-circuit faults detection, classification and location in power transmission lines," *International Journal of Electrical Power and Energy Systems*, vol. 74, pp. 374–383, 2016.

[4] M. Farshad and J. Sadeh, "Fault locating in high voltage transmission lines based on harmonic components of one-end voltage using random forests," *Iranian Journal of Electrical and Electronic Engineering*, vol. 9, pp. 158–166, 2013.

[5] M. Majidi, A. Arabali, and M. Etezadi-Amoli, "Fault location in distribution networks by compressive sensing," *IEEE Transactions on Power Delivery*, vol. 30, no. 4, pp. 1761–1769, 2015.

[6] M. Majidi, M. Etezadi-Amoli, and M. Sami Fadali, "A novel method for single and simultaneous fault location in distribution networks," *IEEE Transactions on Power Systems*, vol. 30, no. 6, pp. 3368–3376, 2015.

[7] S. M. Brahma, "Fault location in power distribution system with penetration of distributed generation," *IEEE Transactions on Power Delivery*, vol. 26, no. 3, pp. 1545–1553, 2011.

[8] J. C. Mayo-Maldonado, J. E. Valdez-Resendiz, D. Guillen et al., "Data-driven framework to model identification, event detection, and topology change location using D-PMUs," *IEEE Transactions on Instrumentation and Measurement*, vol. 69, no. 9, pp. 6921–6933, 2020.

[9] M. R. Shadi, M.-T. Ameli, and S. Azad, "A real-time hierarchical framework for fault detection, classification, and location in power systems using PMUs data and deep learning," *International Journal of Electrical Power and Energy Systems*, vol. 134, Article ID 107399, 2022.

[10] M. Gilanifar, H. Wang, J. Cordova, E. E. Ozguven, T. I. Strasser, and R. Arghandeh, "Fault classification in power distribution systems based on limited labeled data using multi-task latent structure learning," *Sustainable Cities and Society*, vol. 73, Article ID 103094, 2021.

[11] A. Ramtin, V. Hakami, and M. Dehghan, "A self-stabilizing clustering algorithm with fault-containment feature for wireless sensor networks," in *Proceedings of the 7'th International Symposium on Telecommunications (IST'2014)*, pp. 735–739, IEEE, Tehran, Iran, September 2014.

[12] H. Wang, C. Huang, H. Yu, J. Zhang, and F. Wei, "Method for fault location in a low-resistance grounded distribution network based on multi-source information fusion," *International Journal of Electrical Power and Energy Systems*, vol. 125, Article ID 106384, 2021.

[13] A. N. Sheta, G. M. Abdulsalam, and A. A. Eladl, "Online tracking of fault location in distribution systems based on PMUs data and iterative support detection," *International Journal of Electrical Power and Energy Systems*, vol. 128, Article ID 106793, 2021.

[14] M. Hayerikhiyavi and A. Dimitrovski, "Gyrator-capacitor modeling of a continuously variable series reactor in different operating modes," in *Proceeding of the 2021 IEEE Kansas Power and Energy Conference (KPEC)*, pp. 1–5, IEEE, Manhattan, KS, USA, April 2021.

[15] C. G. Arsoniadis, C. A. Apostolopoulos, P. S. Georgilakis, and V. C. Nikolaidis, "A voltage-based fault location algorithm for medium voltage active distribution systems," *Electric Power Systems Research*, vol. 196, Article ID 107236, 2021.

[16] M. Seyedi, S. A. Taher, B. Ganji, and J. Guerrero, "A hybrid islanding detection method based on the rates of changes in voltage and active power for the multi-inverter systems," *IEEE Transactions on Smart Grid*, vol. 12, no. 4, pp. 2800–2811, 2021.

[17] S. Belagoune, N. Bali, A. Bakdi, B. Baadji, and K. Atif, "Deep learning through LSTM classification and regression for transmission line fault detection, diagnosis and location in large-scale multi-machine power systems," *Measurement*, vol. 177, Article ID 109330, 2021.

[18] S. Pourjabar and G. S. Choi, "A high-throughput multimode low-density parity-check decoder for 5G New Radio," *International Journal of Circuit Theory and Applications*, vol. 50, no. 4, pp. 1365–1374, 2022.

[19] F. V. Lopes, A. Mouco, R. O. Fernandes, and F. C. Neto, "Real-World case studies on transmission line fault location feasibility by using M-Class phasor measurement units," *Electric Power Systems Research*, vol. 196, Article ID 107261, 2021.

[20] M. Vahidi Farashah, A. Etebarian, R. Azmi, and R. Ebrahimzadeh Dastjerdi, "An analytics model for TelecoVAS customers' basket clustering using ensemble learning approach," *Journal of Big Data*, vol. 8, no. 1, pp. 36–24, 2021.

[21] F. Abed Azad, S. Ansari Rad, M. R. Hairi Yazdi, M. Tale Masouleh, and A. Kalhor, "Dynamics analysis, offline–online tuning and identification of base inertia parameters for the 3-DOF Delta parallel robot under insufficient excitations," *Meccanica*, vol. 57, no. 2, pp. 473–506, 2022.

[22] A. Mouco and A. Abur, "Improving the wide-area PMU-based fault location method using ordinary least squares estimation," *Electric Power Systems Research*, vol. 189, Article ID 106620, 2020.

[23] V. A. Chenarlogh, F. Razzazi, and N. Mohammadyahya, "A multi-view human action recognition system in limited data case using multi-stream CNN," in *Proceedings of the 2019 5th Iranian Conference on Signal Processing And Intelligent Systems (ICSPIS)*, pp. 1–11, IEEE, Shahrood, Iran, December 2019.

[24] J. J. Chavez, N. V. Kumar, S. Azizi et al., "PMU-voltage drop based fault locator for transmission backup protection," *Electric Power Systems Research*, vol. 196, Article ID 107188, 2021.

[25] S. Hosseini, "Evaluation of Splint Effect on the Dimensional Variations of Implants Location Transfer with A 25° angle by Open Tray Molding Method," *Nveo-Natural Volatiles and Essential Oils Journal| Nveo*, vol. 9, pp. 1122–1145, 2022.

[26] C. Fei, G. Qi, and C. Li, "Fault location on high voltage transmission line by applying support vector regression with fault signal amplitudes," *Electric Power Systems Research*, vol. 160, pp. 173–179, 2018.

[27] A. Rezaee, O. Akbari Sheikhabad, and L. Beygi, "Quality of transmission-aware control plane performance analysis for elastic optical networks," *Computer Networks*, vol. 187, Article ID 107755, 2021.

[28] M. Trik, S. Pour Mozaffari, and A. M. Bidgoli, "Providing an adaptive routing along with a hybrid selection strategy to increase efficiency in NoC-based neuromorphic systems," *Computational Intelligence and Neuroscience*, vol. 2021, Article ID 8338903, 8 pages, 2021.

[29] M. Pignati, L. Zanni, P. Romano, R. Cherkaoui, and M. Paolone, "Fault detection and faulted line identification in active distribution networks using synchrophasors-based real-time state estimation," *IEEE Transactions on Power Delivery*, vol. 32, no. 1, pp. 381–392, 2017.

[30] M. Trik, S. Pour Mozafari, and A. M. Bidgoli, "An adaptive routing strategy to reduce energy consumption in network on chip," *Journal of Advances in Computer Research*, vol. 12, no. 3, pp. 13–26, 2021.

[31] S. Hosseini and B. Khamesee, "BIO-03 design and control of A magnetically driven CAPSULE-ROBOT for endoscopy (Biomedical equipments I, technical program of oral presentations)," in *Proceedings of JSME-IIP/ASME-ISPS Joint Conference On Micromechatronics For Information And Precision Equipment: IIP/ISPS Joint MIPE 2009*, pp. 219-220, The Japan Society of Mechanical Engineers, Shahrood, Iran, June 2009.

[32] R. F. Buzo, H. M. Barradas, and F. B. Leão, "A new method for fault location in distribution networks based on voltage sag measurements," *IEEE Transactions on Power Delivery*, vol. 36, no. 2, pp. 651–662, 2021.

[33] H. Mozaffari and A. Houmansadr, "Heterogeneous private information retrieval," in *Proceedings of the Network and Distributed Systems Security (NDSS) Symposium 2020*, New York, NY, USA, January 2020.

[34] J. Sun, Y. Zhang, and M. Trik, "PBPHS: a profile-based predictive handover strategy for 5G networks," *Cybernetics and Systems*, vol. 40, pp. 1–22, 2022.

[35] M. Dashtdar, S. M. Sadegh Hosseinimoghadam, and M. Dashtdar, "Fault location in the distribution network based on power system status estimation with smart meters data," *International Journal of Emerging Electric Power Systems*, vol. 22, no. 2, pp. 129–147, 2021.

[36] P. Rafiee and G. Mirjalily, "Distributed network coding-aware routing protocol incorporating fuzzy-logic-based forwarders in wireless ad hoc networks," *Journal of Network and Systems Management*, vol. 28, no. 4, pp. 1279–1315, 2020.

[37] M. Trik, A. M. N. G. Molk, F. Ghasemi, and P. Pouryeganeh, "A hybrid selection strategy based on traffic analysis for improving performance in networks on chip," *Journal of Sensors*, vol. 2022, Article ID 3112170, 19 pages, 2022.

[38] D. E. Goldberg, *Genetic Algorithms in Search, Optimization, and Machine Learning*, Addison, Boston, MA, USA, 1989.

[39] S. Radhoush, F. Shabaninia, and J. Lin, "Distribution system state estimation with measurement data using different compression methods," in *Proceedings of the 2018 IEEE Texas Power and Energy Conference (TPEC)*, pp. 1–6, IEEE, College Station, TX, USA, February 2018.

[40] D. A. Coley, *An Introduction to Genetic Algorithms for Scientists and Engineers*, World Scientific Publishing Company, Singapore, 1999.

[41] M. Melanie, "An introduction to genetic algorithms mit press," *Cambridge*, vol. 36, pp. 126–144, 1996.

[42] K. Höschel and V. Lakshminarayanan, "Genetic algorithms for lens design: a review," *Journal of Optics*, vol. 48, no. 1, pp. 134–144, 2019.

[43] H. Mozaffari, A. Houmansadr, and A. Venkataramani, "Blocking-resilient communications in information-centric networks using router redirection," in *Proceedings of the 2019 IEEE Globecom Workshops (GC Wkshps)*, pp. 1–6, IEEE, Waikoloa, HI, USA, December 2019.

[44] E. Khan and P. Venkatapuram, "Neufuz: neural network based fuzzy logic design algorithms," in *Proceedings of the 1993 Second IEEE International Conference on Fuzzy Systems*, pp. 647–654, San Francisco, CA, USA, August 1993.

[45] J. S. Jang, "ANFIS: adaptive-network-based fuzzy inference system," *IEEE transactions on systems, man, and cybernetics*, vol. 23, no. 3, pp. 665–685, 1993.

[46] B. HassanVandi, R. Kurdi, and M. Trik, "Applying a modified triple modular redundancy mechanism to enhance the reliability in software-defined network," *International Journal of Electrical and Computer Sciences*, vol. 3, no. 1, pp. 10–16, 2021.

[47] M. Elsisi, M.-Q. Tran, K. Mahmoud, M. Lehtonen, and M. M. Darwish, "Robust design of ANFIS-based blade pitch controller for wind energy conversion systems against wind speed fluctuations," *IEEE Access*, vol. 9, pp. 37894–37904, 2021.

[48] J. Akhavan and S. Manoochehri, "Sensory data fusion using machine learning methods for in-situ defect registration in additive manufacturing: a review," in *Proceedings of the 2022 IEEE International IOT, Electronics And Mechatronics Conference (IEMTRONICS)*, pp. 1–10, IEEE, Waikoloa, HI, USA, June 2022.

[49] M. Vahidi Farashah, A. Etebarian, R. Azmi, and R. Ebrahimzadeh Dastjerdi, "A hybrid recommender system based-on link prediction for movie baskets analysis," *Journal of Big Data*, vol. 8, no. 1, pp. 32–24, 2021.

[50] C.-T. Lin and C. Lee, *Neural Fuzzy Systems: A Neuro—Fuzzy Synergism to Intelligent Systems*, Prentice-Hall, Englewood Cliffs, NJ, 1996.

[51] M. Trik, A. M. Bidgoli, H. Vashani, and S. P. Mozaffari, "A New Adaptive Selection Strategy for Reducing Latency in Networks on Chip," *Integration*, vol. 89, 2022.

[52] M. Sugeno and K. Tanaka, "Successive identification of a fuzzy model and its applications to prediction of a complex system," *Fuzzy Sets and Systems*, vol. 42, no. 3, pp. 315–334, 1991.